

Time resolved optical Kerr effect analysis of urea–water system

A. Idrissi^{a)}

Laboratoire de Spectrochimie Infrarouge et Raman (LASIR UPR A2632L), Centre d'Etudes et de Recherches Lasers et Applications, Université des Sciences et Technologies de Lille, 59650 Villeneuve d'Ascq Cedex, France

P. Bartolini

European Laboratory for Non-linear Spectroscopy (LENS), 2, Largo Fermi, 50125 Florence, Italy and Università di Firenze, Dipartimento di Chimica, Via G. Capponi 9, 50121 Firenze, Italy

M. Ricci

European Laboratory for Non-linear Spectroscopy (LENS), 2, Largo Fermi, 50125 Florence, Italy and Università della Basilicata, Dipartimento di Chimica, Via N. Sauro, 85100 Potenza, Italy

R. Righini

European Laboratory for Non-linear Spectroscopy (LENS), 2, Largo Fermi, 50125 Florence, Italy and Università di Firenze, Dipartimento di Chimica, Via G. Capponi 9, 50121 Firenze, Italy

(Received 14 June 2000; accepted 19 January 2001)

The nuclear dynamics of urea aqueous solution was analyzed by time resolved optical Kerr effect (OKE). The data analysis was achieved in time and in frequency domains. Three relaxation times characterize the time decay of the OKE signal at high mole fractions of urea, while only two relaxation times characterize this decay for the low mole fractions. The observed slowest relaxation time increases with increasing the mole fraction of urea. The comparison between this relaxation time and the ones determined by Raman and nuclear magnetic resonance spectroscopies suggests that the slow relaxation time is related to the reorientation of an axis lying in the plane of the urea molecule. At high mole fractions, the power spectra derived from the Fourier transform of the OKE signal are characterized by one broad peak at around 70 cm^{-1} and by a shoulder at around 160 cm^{-1} in the high frequency part of the former peak. This shoulder is related to the hydrogen bond interactions which involve urea molecules. Molecular dynamics simulation results on urea/water system suggest that the power spectra derived from OKE data could be interpreted in terms of translational motions (caging effect) and in terms of rotational motion (libration) of urea molecules.

© 2001 American Institute of Physics. [DOI: 10.1063/1.1355019]

I. INTRODUCTION

The importance of urea/water solution is due to the properties of this solution in biological studies. In fact, at high urea concentration (higher than 4 mol L^{-1}) the solution has the effect of a denaturant of proteins (from helix form to coil)¹ and the effect of an inhibitor of micellar aggregation.² Two models were developed to describe urea's aqueous solution properties. The SKSS model³ describes those properties in terms of the ability of urea molecules to form hydrogen bonds to give dimers or oligomers of urea molecules (in this model, the water–water and urea–water interactions are neglected). The second model known as the Frank–Franks (FF) model⁴ associates these properties with the changes in water structure. In the later model, the water exists in two states which are in equilibrium, namely the solid icelike structure and the free water molecule structure. The effect of urea is to move the equilibrium between the two structures to the free water molecule structure. Both of the two models explain the experimental thermodynamic properties of the solution characterized by a large enthalpy change ($+15\text{ kJ mol}^{-1}$) and a small free energy change.⁵ Many experimen-

tal and theoretical techniques were used to study this system. The interpretation of these results was made in the frame of the two previous models. The low frequency Raman experiment⁶ has demonstrated that urea is a “structure breaker” of water. The nuclear magnetic resonance (NMR) experiment,⁷ the Raman spectroscopy experiment,⁸ the x-ray experiment,⁹ and the calorimetric experiment¹⁰ show no evidence of the urea dimer. These experiments support the FF model. However, the osmotic pressure experiment¹¹ demonstrates the existence of urea oligomers in solution. Results obtained by other techniques prove neither of the two models. In fact, a dielectric relaxation experiment¹² reports two slightly different relaxation times for pure water and for water in urea solutions; no dimers of urea were found. Neutron diffraction analysis¹³ of urea/D₂O showed that urea does not change water structure appreciably. Results from molecular dynamics simulation results show that the overall water–water radial distribution functions are not strongly affected by the urea concentration¹⁴ and no evidence of urea dimers was found.

We undertake an analysis of the urea/water system by the resolved time optical Kerr effect (OKE). This technique has the advantage of analyzing the data by using both the model-dependent approach (exponential decay in general),

^{a)}Electronic mail: nacer.idrissi@univ-lille1.fr

which assumes distinct temporal responses, and the model-independent Fourier transform approach, which generates a power spectrum. The analysis in the time domain makes it possible to identify the different components in the multiexponential decay and to assign physical meaning to them. The second approach allows the comparison with DLS, low frequency Raman, and far-infrared spectroscopies.

As pointed out in previous work,^{15,16} the role of the local environment in determining the intermolecular structure and dynamics of liquids can be revealed in a controlled manner through dilution studies. In consequence, the analysis of the urea/water system was extended to include the effect of the concentration of urea on the structural and dynamical properties of the system. In fact, the denaturation effect of urea occurs at high concentrations, and hence it is possible that quite different molecular mechanisms could be involved at low and high mole fractions of urea.

II. EXPERIMENT

The solution was used right after preparation. The sample was placed in a 2 mm quartz cuvette. The specifications of the experimental apparatus have been described in detail previously.¹⁶ The femtosecond OKE measurements were carried out by the use of 60 fs linearly polarized optical pulses centered at 805 nm. The pulses were generated by a laser system consisting of a Kerr lens Ti:sapphire mode-locked oscillator (20 fs pulses) and of a Nd-YLF pumped Ti:sapphire regenerative amplifier (BMI Alpha-1000US), delivering 600 μ J, 60 fs pulses at the repetition rate of 1 kHz. Part of the output beam was split off and directed to the experiment area. About 20% of that beam was used as the probe beam, after passing through a computer controlled delay line. The pump and probe beams which were polarized at 45° with respect to each other, were focused on to the sample by a 600 mm lens (L1). The probe beam crossed a polarizer (P1), a quarter wave plate ($\lambda/4$), the sample, and a second polarizer (P2). To obtain a heterodyne signal the $\lambda/4$ plate was rotated by about 3°, yielding an out-of-phase oscillation, so that the real (birefringence) and the imaginary (dichroism) parts of the nonlinear response are both present in the recorded signal. The latter contribution was verified to be negligible for the solutions investigated by performing an in-phase OHD measurement (i.e., by rotating the analyzer polarizer P2).

The pure heterodyne signal was obtained as the difference between two scans made with the $\lambda/4$ plate rotated by the same angle in opposite directions. The detection system consisted of two large area photodiodes and a differential amplifier. The output of the amplifier was collected by a boxcar-gated integrator and sent to the computer. To estimate the base line, the response function was measured up to 41 ps for the high mole fractions and up to 10 ps for the low mole fractions of urea.

Data analysis procedure. The signal measured in a heterodyne detected OKE experiment is proportional to the material response function. Our data analysis was achieved in time and frequency domains. The time domain analysis was used when there is no doubt about the exponential decay of

the signal. We fitted the long time part of the OKE relaxation to a multiexponential function of the type

$$R(t) = \sum_{i=1} A_i \exp\left(-\frac{t}{\tau_i}\right) (1 - \exp(-2t/\beta)). \quad (1)$$

The relaxation time τ_i characterizes the process involved in the response $R(t)$ of the system. A_i is the amplitude of the contribution to the response $R(t)$. β is the rise time, it is introduced phenomenologically to account for a delayed onset of the diffusion. As it was demonstrated in previous work,¹⁷ the particular choice of β has only a minor influence on the shape of the remaining signal.

A frequency domain analysis was used for the signal of the OKE after subtraction of the contribution at long time. This analysis is based on a recent Fourier transform technique.¹⁸ It enables both the separation of nuclear contributions from electronic contributions to the Kerr signal and the deconvolution of the instrument response (the cross correlation in time between the probe and pump pulses) from the molecular response function. In fact, the time-dependent response, $T(\tau)$, measured in the OKE experiment, is a convolution of the nonlinear response function $R(t)$, with the instrument response $G^{(2)}(t)$,

$$T(\tau) \propto \int_{-\infty}^{+\infty} R(t-\tau) G^{(2)}(t) dt. \quad (2)$$

The response function $R(t)$ is a result of the electronic $R_e(t)$ and nuclear $R_n(t)$ contributions. The separation between the two contributions is achieved by means of the following facts: the electronic contribution has short time duration. It is symmetric relative to time zero. Thus, its contribution is present only in the real part of the Fourier transform of relation (1), while the nuclear contribution is the only one present in the imaginary part. Thus, we have the following relations where FT designates the Fourier transform:

$$\Xi(\bar{\nu}) = \int_{-\infty}^{+\infty} R(t) e^{i2\pi c \bar{\nu} t} dt, \quad (3)$$

$$\Xi(\bar{\nu}) = \frac{\text{FT}[T(t)]}{\text{FT}[G^{(2)}(t)]}, \quad (4)$$

$$\text{Im}[\Xi(\bar{\nu})] = \text{Im FT}[R(t)], \quad (5)$$

where $\text{Im}[\Xi(\bar{\nu})]$ is the power spectrum and reflects only the nuclear contribution.

III. RESULTS AND DISCUSSION

The resolved time OKE signal of urea/water at different concentration is presented in Fig. 1. All the signals were normalized to allow comparison between them. Figure 1 shows that the decay of the signal is exponential for delay times longer than 2 ps. At short time, the time profile is definitely not exponential. Two striking features should be noticed. First, at short time, the decay time increases with increasing mole fraction of urea (see the inset in Fig. 1). Second, the signal at about 100 fs presents a shoulder for values of mole fraction greater than 0.13. The first conclusion is that the dynamics of urea molecules in the range of

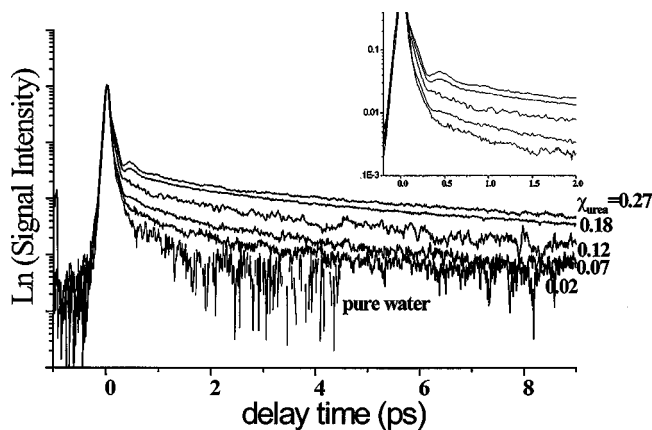


FIG. 1. The time resolved OKE signal of urea/water at different mole fractions of urea.

mole fraction $0.01 < \chi_{\text{urea}} < 0.12$, which will be referred to as low mole fractions, is different from that corresponding to the mole fraction range of $0.13 < \chi_{\text{urea}} < 0.27$, which will be referred to as high mole fractions.

A. Time domain analysis

A nonlinear curve fitting based on Marquardt algorithm was used to characterize the different relaxation processes involved in the decay of the OKE signal. We found that three exponential functions fit the OKE signal reasonably well in the range of $0.13 < \chi_{\text{urea}} < 0.27$ while only two exponential functions fit the OKE signal well in the range $0.01 < \chi_{\text{urea}} < 0.11$. In Fig. 2, we report the relaxation times obtained by the fitting procedure for all the mole fractions studied.

The slow relaxation time τ_3 increases slowly in the low mole fraction range, whereas it increases rapidly in the high mole fraction range. The relaxation time τ_2 appears for $\chi_{\text{urea}} > 0.11$. It increases with increasing χ_{urea} . The relaxation time τ_1 is almost constant in the whole range of urea mole fraction.

It is generally accepted that the long time decay of the Kerr signal is related to the reorientational diffusion motion of the molecules. The hydrodynamic theory relates the reori-

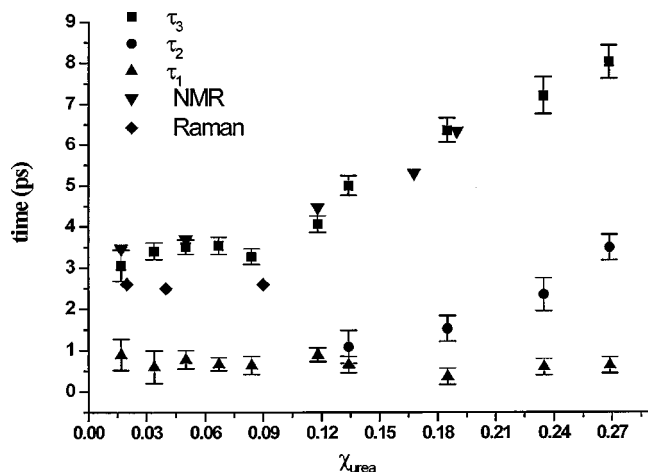


FIG. 2. The relaxation times obtained by the fitting procedure for all the mole fractions studied.

entational relaxation time to the macroscopic viscosity η of the liquid, considering molecular reorientation as a diffusive process driven by thermal energy and controlled by hydrodynamic friction. This results in the well-known Stokes–Einstein–Debye relation:

$$\tau = fCV_M \frac{\eta}{kT} + \tau_0, \quad (6)$$

where V_M is the molecular volume and f and C represent a form factor and a factor reflecting the hydrodynamic boundary condition, respectively. τ_0 is an additive term usually introduced *ad hoc* in this equation to account for the nonzero value of τ at the extrapolated limit of the ratio η/T . τ_0 is identified with the free rotor relaxation time. The expression of the factor f could be calculated analytically for reorienting objects if their shape is sufficiently symmetric.¹⁹ It is clear that in the frame of these approximations, only one reorientation relaxation time is observed. However, the diffusive reorientation of unsymmetrical, ellipsoidal molecules is expected to consist of a sum of exponential terms. They are associated with the reorientation of the principal axes of the molecule. In the most general case of a completely asymmetric body, five exponential terms appear to account for the reorientation relaxation.²⁰ By assuming certain symmetry properties of the molecule, the reorientation could be described by three relaxation times. In fact, a result on halogen-substituted benzene²¹ has demonstrated diffusive rotational motion about more than one molecular axis. The evidence of the reorientation along two distinct axes has already been observed in halobenzene,²² poly-phenyls,²³ aniline,²⁴ and benzonitrile.²⁵ Younggreen and Acrivos²⁶ treated the rotational motion of an ellipsoidal with three different principal axes and they derived three different effective volumes and two relaxation times for any given ellipsoid. According to these facts, the different relaxation times observed in our experiment could be related to the reorientation of the principal axes of the urea molecules. The comparison of these relaxation times with those obtained by Raman and NMR techniques is not obvious, because, in general, only one reorientational relaxation time is reported. To carry out this comparison, one should clarify the following points. First, one has to define the precise axis whose reorientation is considered. Second, one should identify the nature of the reorientational relaxation time given by the technique used which could be collective or single particle. Considering the last point, it is generally admitted that Raman and NMR spectroscopies give information on the single reorientation correlation time. Thus, a direct comparison between our OKE data and those obtained by Raman and NMR spectroscopies is not possible because of the collective nature of the reorientational relaxation time given by the OKE. Despite this fact, some information can be drawn from the direct comparison between the OKE relaxation time and single particle reorientation relaxation times (Raman, NMR) given in Fig. 2. Results from band shape analysis⁸ of the CN stretching frequency have shown that the reorientational relaxation is almost constant in the mole fraction range between 0.02 and 0.09, and the value of 2.6 ps was reported. This time corresponds to the reorientation of a unit vector along the CN

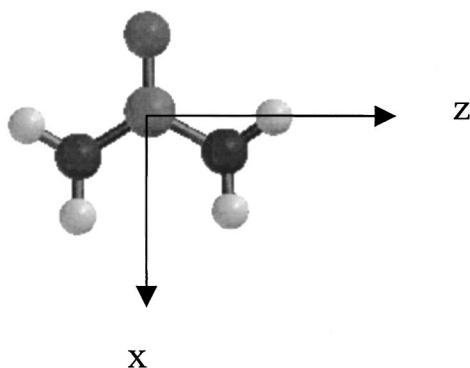


FIG. 3. Geometry of urea molecule.

axis. The CN axis lies in the plane of the urea molecule (see Fig. 3). The values of the relaxation time obtained by Raman spectroscopy are close to the reorientation relaxation time τ_3 determined by OKE. This result suggests that the relaxation time τ_3 is related to the reorientation along an axis in the plane of the urea molecule.

The reorientational relaxation times of urea in water molecules obtained from ^{14}N NMR studies of aqueous urea solution⁷ were extrapolated from Fig. 2 in this reference and superposed to the corresponding time obtained by OKE. The ^{14}N NMR spin-lattice relaxation time is most strongly weighted by the axis, which reorients the N–H bond most quickly. The N–H axis lies in the plane of the urea molecule (see Fig. 3). This result also suggests that the relaxation time τ_3 is related with a reorientation about a principal axis, which lies in the plane of the urea molecule.

The direct comparison between τ_3 obtained by OKE and the corresponding time obtained by NMR and Raman spectroscopies indicates also that there is almost no correlation of reorientational motion along a unit vector in the plane between two different urea molecules in all the mole fractions of urea.

To obtain further insight into the microscopic reorientation process, the autocorrelation function of the unit vector along the principal axes of the urea molecule was calculated by molecular dynamics simulation:²⁷

$$C_2^\alpha(t) = \langle P_2(\mathbf{u}_i^\alpha(0) \cdot \mathbf{u}_i^\alpha(t)) \rangle, \quad (7)$$

where i labels the molecule, and $\alpha = x, y, z$. The unit vectors $\mathbf{u}^x, \mathbf{u}^y, \mathbf{u}^z$ are defined in Fig. 3. P_2 is the second Legendre polynomial

$$P_2(\mathbf{u}_1 \cdot \mathbf{u}_2) = \frac{3}{2} \cos^2(\angle u_1 u_2) - \frac{1}{2}. \quad (8)$$

As shown in Fig. 4, the reorientation of the urea molecule is more hindered at the high mole fractions than at the low mole fractions of urea. At all mole fractions, the reorientation of the principal axes lying in the plane of the urea molecule is more hindered than that of the perpendicular axis to that plane. This result suggests that the relaxation time τ_3 obtained by OKE measurement could be related to the reorientation of an axis which lies in the plane of the urea molecule, while the reorientation time τ_2 could be related to the reorientation of an axis perpendicular to this plane. It is interesting to notice that the short time (<0.5 ps) behavior of

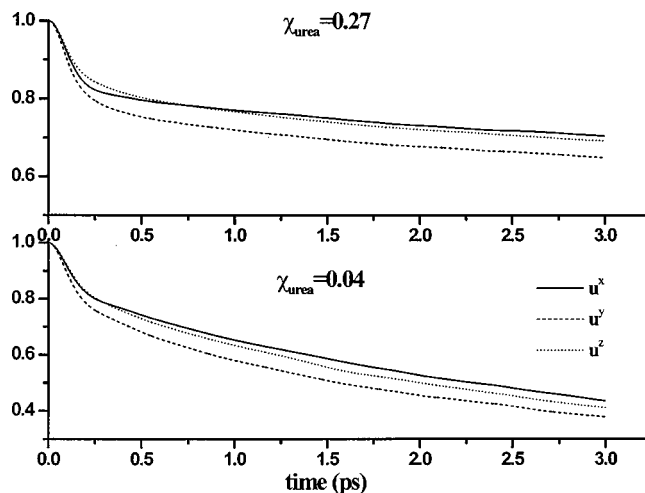


FIG. 4. The reorientational correlation functions of the principal axes of the urea molecule.

the reorientation dynamics of urea molecule is anisotropic in high mole fraction in comparison to the one in the low mole fraction. This anisotropy is also suggested by the comparison of the correlation time associated with the reorientation of urea molecule along its principal axes in the low and high mole fractions (see Table IX of Ref. 27). It is expected that the reorientation dynamics of urea molecules is influenced by the hydrogen bond interactions. These later interactions are known to be directional and could explain the anisotropy observed in the short time reorientation dynamics.

B. Frequency domain analysis

The power spectra $\text{Im}[\Xi(\bar{\nu})]$ of urea/water solution were derived from the OKE data by using the Fourier transform technique by using Eqs. (4) and (5). First, we subtract the different diffusive contributions to the OKE signal. These operations are illustrated for $\chi_{\text{urea}} = 0.27$ in Figs. 5(a)–5(c). The power spectra $\text{Im}[\Xi(\bar{\nu})]$ were obtained by the Fourier

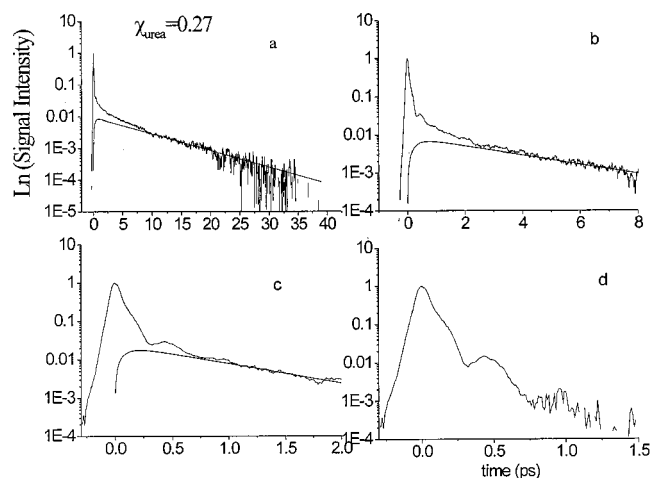


FIG. 5. The different steps to obtain the time behavior of the nondiffusive part of OKE signal for $\chi_{\text{urea}} = 0.27$. The subtraction of the different diffusive contributions to the OKE signal. These operations are illustrated for $\chi_{\text{urea}} = 0.27$ in (a)–(c). (d) The time profile of the OKE signal after the subtraction of the different diffusive contributions.

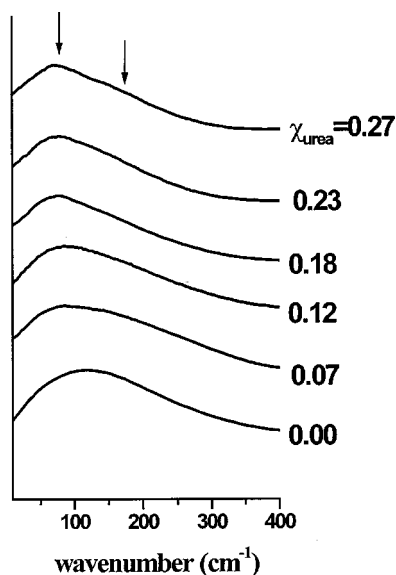


FIG. 6. The imaginary part obtained by Fourier transform of the OKE signal for different mole fractions of urea.

transform of the remainder experimental data shown in Fig. 5(d). The spectral resolution is about 16.7 cm^{-1} . The fine tuning of the relative time origins of $T(t)$ (the experimental OKE data after subtraction of the exponential long time decay) and $G^{(2)}(t)$ in Eq. (4) was achieved using the fact that the final spectrum was positive in all the frequency range considered (400 cm^{-1}), with vanishing intensity at its high frequency end. The power spectra $\text{Im}[\Xi(\bar{\nu})]$ as a function of the mole fractions of urea are presented in Fig. 6. At high mole fractions, the $\text{Im}[\Xi(\bar{\nu})]$ is characterized by one broad peak at around 70 cm^{-1} and by a shoulder at around 160 cm^{-1} in the high frequency part of the former peak. At low mole fractions,²⁸ the $\text{Im}[\Xi(\bar{\nu})]$ is characterized by one asymmetric broad peak at around 70 cm^{-1} . A curve fitting procedure using a Gaussian function reveals that two bands contribute to this asymmetric peak, centered, respectively, at around 70 and 200 cm^{-1} . The power spectrum of water is also included in Fig. 6. It is characterized by an asymmetric broad peak centered at around 110 cm^{-1} which is decomposed by a curve fitting procedure in two contributions, centered, respectively, at around 80 and 190 cm^{-1} . Previous work²⁹ on water using a time resolved OKE with a pulse width as short as 38 fs has shown that the power spectrum of water is composed of two well-resolved peaks at 40 and 165 cm^{-1} , respectively. The discrepancy between the power spectra obtained from the former experiment and our OKE experiment could be related to the difference in the pulse width used in the two experiments. In fact, it was shown that the pulse width has a spectral-filter effect on the intrinsic frequency response of the medium.^{17(a)} This means that only the vibrational modes (associated with intermolecular or intramolecular interactions) within the coherent bandwidth of the laser pulses are efficiently excited by stimulated Raman mechanism. Thus, the higher frequency part of the power spectra is underestimated by this filter effect. This could explain that the power spectrum of pure water derived from the OKE data is not resolved in two clear distinct peaks. In con-

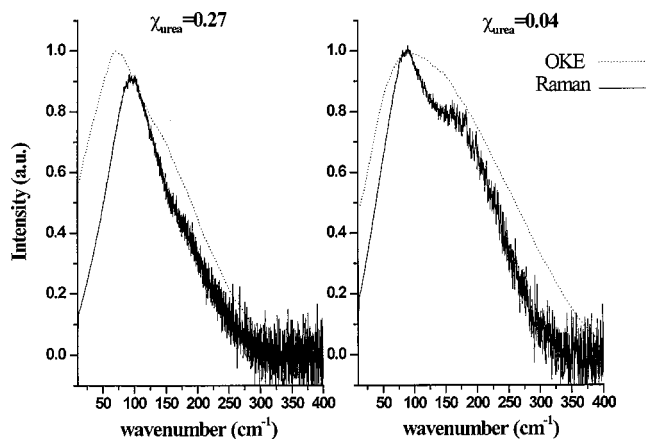


FIG. 7. The low frequency Raman spectra of urea/water solution in the so-called reduced from $\tilde{R}(\bar{\nu})$ and the power spectra obtained by Fourier transform of the OKE signal.

sequence our frequency domain data provide analysis in the frame of this limitation. The comparison between the low frequency Raman spectrum of urea/water solution in the so-called reduced from $\tilde{R}(\bar{\nu})$ and $\text{Im}[\Xi(\bar{\nu})]$ is given for $\chi_{\text{urea}} = 0.04$ and 0.27 in Fig. 7. One notices that the shapes of $\text{Im}[\Xi(\bar{\nu})]$ and $\tilde{R}(\bar{\nu})$ are similar at $\chi_{\text{urea}} = 0.27$. The peak and its shoulder maximum in $\text{Im}[\Xi(\bar{\nu})]$ are located at lower frequencies with respect to those of $\tilde{R}(\bar{\nu})$. At $\chi_{\text{urea}} = 0.04$, two peaks at, respectively, 60 and 190 cm^{-1} are present in $\tilde{R}(\bar{\nu})$. However, only one asymmetric broad peak is present in $\text{Im}[\Xi(\bar{\nu})]$. As pointed out before, this peak is decomposed by a curve fitting procedure in two contributions, centered at 70 and 200 cm^{-1} , respectively.

In the case of a liquid mixture, it is more difficult (than for pure liquid) to rationalize the nature and the origin of the OKE signal. One should cope with the fundamental problems of a large number of different interaction mechanisms and their cross terms which contribute to the OKE signal, in fact, in our case, the intermolecular interactions (urea-urea, urea-water, and water-water) modulate the susceptibility of the solution. To make a hypothesis on the main contribution to the OKE signal, we take in to account the following facts. For a series of nitrile solvents,³⁰ it was demonstrated that the contribution to the Kerr signal strongly correlates with the degree of differences in principal polarizabilities of the individual molecules, the more anisotropic in polarizability, the more intermolecular contribution is present in the optical Kerr response. The degree of anisotropy is directly reflected by the factor κ , which is given by

$$\kappa^2 = \frac{1}{6\alpha^2} [(\alpha_1 - \alpha)^2 + (\alpha_2 - \alpha)^2 + (\alpha_3 - \alpha)^2], \quad (9)$$

where $\alpha_1, \alpha_2, \alpha_3$ are the polarizabilities in the three directions of the principal axes and α is the average mean polarizability. The values of κ for water and urea are 0.069 and 0.255 , respectively. The different values of polarizability for urea were taken from Ref. 30. This result shows that the degree of anisotropy of the urea molecule is almost four times higher than the one corresponding to water molecule. Furthermore, the nonlinear coefficient of urea in aqueous so-

lution of urea³¹ is seven times greater than the corresponding one to water. Thus, in our analysis, we made the hypothesis that the shoulder, which appears in $\text{Im}[\Xi(\bar{\nu})]$, at high mole fractions of urea could be an expression of the hydrogen bond intermolecular interactions which involve urea molecule. More information is needed to identify whether these interactions are due to the hydrogen bond between urea and water molecules or between urea and urea molecules (dimers).

It is known that the different motions of urea molecules (reorientation, rotation, and translation) have different characteristic times, and it is interesting to find out to which frequency domain they contribute. Thus, we have carried out a molecular dynamics simulation on the urea/water system. The following correlation functions $C_2(t)$, $\Omega(t)$, and $\Psi(t)$ were calculated. These functions are associated with the reorientation, rotation, and translation motions of urea molecules, respectively. The corresponding power spectra obtained by the Fourier transform of these functions were calculated in order to compare them with $\text{Im}[\Xi(\bar{\nu})]$.

$C_2(t)$ is the autocorrelation function of the unit vector along the axis of the dipole moment of the urea molecule. This function was calculated using Eqs. (8) and (9). The power spectrum is given by the Fourier transform (FT) $\tilde{C}_2(\bar{\nu}) = \text{FT}[C_2(t)]$. $\tilde{C}_2(\bar{\nu})$ was calculated as follow: First, we fit the long time decay of $C_2(t)$ by an exponential function. Second, the long time contribution is removed by subtracting the exponential decay from $C_2(t)$. Thus, doing this operation, it is the short time dynamics of the reorientation which contributes to $\tilde{C}_2(\bar{\nu})$.

The angular velocity autocorrelation function $\Omega(t)$ is given by

$$\Omega(t) = \langle \omega(t) \cdot \omega(0) \rangle, \quad \tilde{\Omega}(\bar{\nu}) = \text{FT}[\Omega(t)]. \quad (10)$$

The velocity autocorrelation function of the center of mass of water molecule is given by

$$\Psi(t) = \langle \mathbf{v}(t) \cdot \mathbf{v}(0) \rangle, \quad \tilde{\Psi}(\bar{\nu}) = \text{FT}[\Psi(t)]. \quad (11)$$

The comparison of the calculated power spectra from molecular dynamics and $\text{Im}[\Xi(\bar{\nu})]$ is shown in Fig. 8. It appears that the reorientational (short time), rotational dynamics of the urea molecule contribute in almost the same frequency domain. This shows the equivalence between the two dynamics. The contribution of the translation and rotation movements of the urea molecule lies in the same frequency domain as that of $\text{Im}[\Xi(\bar{\nu})]$. Accordingly, the power spectra $\text{Im}[\Xi(\bar{\nu})]$ could be interpreted in terms of translational dynamics (caging effect) and in terms of rotational dynamics (libration) of urea molecules. This gives a transparent way of interpreting the power spectra derived from OKE data. This interpretation is related to the generally used interpretation based on the interaction-induced dipoles. In fact, the power spectrum is regarded as due to modulation of the susceptibility by intermolecular interactions (interaction-induced dipoles). The susceptibility is given by

$$\tilde{\chi}(t) = \sum_i \tilde{\alpha}_i + \sum_i \sum_{j \neq i} \tilde{\alpha}_i \cdot \vec{T}_{ij} \cdot \tilde{\alpha}_j, \quad (12)$$

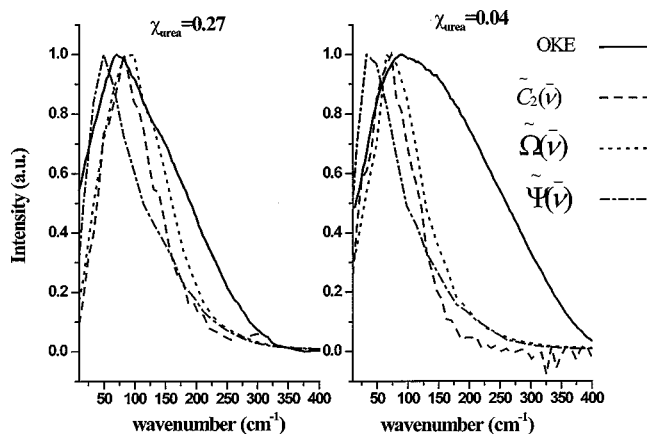


FIG. 8. The comparison of the power spectra derived from the OKE data and the ones obtained by molecular dynamics simulations for the reorientation [$\tilde{C}_2(\bar{\nu})$], rotation [$\tilde{\Omega}(\bar{\nu})$], and translation [$\tilde{\Psi}(\bar{\nu})$] motions of urea (see the text).

where $\tilde{\alpha}_i$ is the polarizability of a single molecule i in the laboratory frame and \vec{T}_{ij} is the dipole–dipole interaction tensor between molecules i and j . \vec{T}_{ij} depends on the translational parameters of the molecule and $\tilde{\alpha}_i$ is modulated through a rotational movement of the molecule.

Analysis of the results obtained by OKE, those obtained by molecular dynamics simulation, and those obtained by low frequency Raman spectra is in progress to interpret the different correlation times observed and the change observed in the power spectra (the position and the width) with increasing the mole fraction of urea. This analysis will help to understand the particular properties of the urea/water system.

IV. CONCLUSIONS

In summary, the nuclear dynamics of the urea molecule in aqueous solution was analyzed by time resolved optical Kerr effect. A multiexponential decay characterizes the time decay of the OKE signal. The comparison between the relaxation times derived by the OKE data, those obtained from the Raman, and NMR spectroscopies suggest that the slowest relaxation time is related to the reorientation of an axis in the plane of the urea molecule. The analysis of the short time reorientational dynamics of the principal axes of urea molecule suggests an increase of anisotropy when the mole fraction of urea increases. This anisotropy is a result of highly directional hydrogen bonding interactions.

The power spectra derived from the OKE show that the low mole fractions are characterized by one sole asymmetric peak, while at high mole fraction, a shoulder appears at around 160 cm^{-1} in the high frequency part of the former peak. Molecular dynamics simulation results on the urea/water system suggest that these power spectra could be interpreted in terms of translational motions (caging effect) and in terms of rotational motion (libration) of urea molecules.

ACKNOWLEDGMENTS

The authors acknowledge Dr. F. Sokolic and Dr. R. Tori for their helpful discussions and suggestions. This work was supported by the Commission of the European Community under Contract No. ERBFMGECT-95-0017 Institut du Développement et des Ressources en Informatique Scientifique is thankfully acknowledged for the CPU time allocation on the C98 machines. The Center d'Études et de Recherches Lasers et Applications is supported by the following organizations, Ministère Chargé de La Recherche, Région Nord/Pas de Calais, and Les Fonds Européen de Développement Economique des Régions.

- ¹J. F. Brandts and L. J. Hunt, *J. Am. Chem. Soc.* **89**, 4826 (1967); G. I. Makhatadze and L. J. Privalov, *J. Mol. Biol.* **226**, 491 (1967).
- ²M. J. Shick, *J. Phys. Chem.* **68**, 3585 (1964).
- ³J. A. Schellman, *Comp. Rend. Trav. Lab. Carlsberg, Ser. Chim.* **29**, 223 (1955); G. C. Kreschek and H. A. Scheraga, *J. Phys. Chem.* **69**, 1704 (1965); R. H. Stokes, *Aust. J. Chem.* **20**, 2087 (1967).
- ⁴H. S. Frank and F. Franks, *J. Chem. Phys.* **48**, 4746 (1968).
- ⁵L. J. Gosting and D. F. Akeley, *J. Am. Chem. Soc.* **74**, 2058 (1952).
- ⁶G. E. Walrafen, *J. Chem. Phys.* **44**, 2726 (1966).
- ⁷E. G. Finer, F. Franks, and M. J. Tait, *J. Am. Chem. Soc.* **94**, 4424 (1972).
- ⁸X. Hoccart and G. Turrell, *J. Chem. Phys.* **99**, 8498 (1993).
- ⁹R. Adams, H. H. M. Balyuzi, and R. E. Burge, *J. Appl. Crystallogr.* **10**, 256 (1977).
- ¹⁰M. Bloemental and G. Somsen, *J. Am. Chem. Soc.* **107**, 3426 (1985); H. Piekarski and G. Somsen, *Can. J. Chem.* **64**, 1721 (1986).
- ¹¹G. Jakli and A. V. A. Van Hook, *J. Phys. Chem.* **85**, 3480 (1981).
- ¹²U. Kaatz, H. Gerke, and R. Pattel, *J. Phys. Chem.* **90**, 5464 (1986).
- ¹³J. L. Finey, A. K. Soper, and J. Turner, *Physica B & C* **151**, 156 (1989); J. Turner, J. L. Finey, and A. K. Soper, *Z. Naturforsch., A: Phys. Sci.* **46a**, 73 (1991).
- ¹⁴E. S. Boek and W. J. Briels, *J. Chem. Phys.* **98**, 1422 (1993); J. H. Cobos, O. Blakeare, M. B. Marin, and M. Bello, *ibid.* **99**, 9122 (1993); H. Tanaka, H. Touhara, K. Nakanishi, and N. Watanabe, *ibid.* **80**, 5170 (1984).
- ¹⁵D. McMorrow, N. Thantu, J. S. Melinger, S. K. Kim and W. T. Lotshaw, *J. Phys. Chem.* **100**, 10389 (1996).
- ¹⁶A. Idrissi, M. Ricci, P. Bartolini, and R. Righini, *J. Chem. Phys.* **111**, 4148 (1999).
- ¹⁷D. McMorrow and W. T. Lotshaw, *Chem. Phys. Lett.* **201**, 369 (1993).
- ¹⁸(a) D. McMorrow and W. T. Lotshaw, *Chem. Phys. Lett.* **174**, 85 (1990); (b) D. McMorrow, *Opt. Commun.* **86**, 236 (1991).
- ¹⁹F. Perrin, *J. Phys. Radium V*, 497 (1934); C. M. Hu and R. Zwanzig, *J. Chem. Phys.* **63**, 3896 (1975).
- ²⁰T. Tao, *Biopolymers* **8**, 609 (1969).
- ²¹D. McMorrow and W. T. Lotshaw, *Proc. SPIE* **981**, 20 (1988).
- ²²M. Neelakandam, D. Pant, and E. L. Quivetis, *J. Phys. Chem.* **101**, 2936 (1997).
- ²³R. Torre, I. Santa, and R. Righini, *Chem. Phys. Lett.* **212**, 90 (1993); F. W. Deeg, J. J. Stankus, S. R. Greenfield, V. J. Newell, and M. D. Fayer, *J. Chem. Phys.* **90**, 6893 (1989).
- ²⁴N. A. Smith, S. Lin, S. R. Meech, and K. Yoshihara, *J. Phys. Chem.* **101**, 9578 (1997).
- ²⁵P. Cong, H. P. Deul, and J. D. Simon, *Chem. Phys. Lett.* **240**, 72 (1995).
- ²⁶G. K. Younggreen and A. Acrivos, *J. Chem. Phys.* **63**, 3846 (1975).
- ²⁷A. Idrissi, F. Sokolic, and A. Perera, *J. Chem. Phys.* **112**, 9479 (2000).
- ²⁸S. Palese, L. Shilling, R. J. D. Miller, P. R. Staver, and W. T. Lotshaw, *J. Phys. Chem.* **98**, 6308 (1994).
- ²⁹P. Cong, J. D. Simon, and Y. Yan, *Ultrafast Processes in Chemistry and Photobiology*, edited by M. A. El-Sayed, I. Tanaka, and Y. Molin (Blackwell Science, 1995), p. 78; H. P. Deuel, P. Cong, and J. D. Simon, *J. Phys. Chem.* **98**, 12600 (1994).
- ³⁰H. Reis, G. Papadopoulos, and R. W. Munn, *J. Chem. Phys.* **109**, 6828 (1998).
- ³¹I. Ledoux and J. Zyss, *Chem. Phys.* **73**, 203 (1982).